Vector decay constants in quarkonia

B.D. Jones* and R.M. Woloshyn

TRIUMF, 4004 Wesbrook Mall, Vancouver, British Columbia, Canada, V6T 2A3

Lattice NRQCD with leading finite lattice spacing errors removed is used to simulate heavy-heavy vector decay constants. Quenched simulations are performed at three values of the coupling and fifteen values of the quark mass. The improved gauge action with plaquettes and rectangles is used. Landau link improvement is used throughout. "Perturbative" and nonperturbative meson masses are compared. One-loop perturbative matching between lattice and continuum heavy-heavy vector currents is performed. The data is consistent with $af_V \propto \sqrt{M_V\,a}$.

1. INTRODUCTION

The gross features of heavy quarkonia are well described by lattice NRQCD [1–3]. However, spin splittings (which are small for quarkonia) tend to be underestimated—even when relativistic corrections are included [4]. Spin splittings are one measure of the mesonic wave function at the origin; another is the vector meson decay constant.

A previous study [5] of the vector decay constant found large corrections from the perturbative matching between the continuum and lattice matrix elements. Another study [6] reported a rather imprecise value for simulations with the order v^2 classically improved vector current. In this paper, we try to improve these calculations by removing the leading finite lattice spacing errors in the fermion and gauge actions in a symmetric fashion and by performing a more precise simulation with the inclusion of the order v^2 classically improved current.

1.1. Lattice NRQCD

The fermion Lagrangian is discretized in a symmetric fashion with the leading finite lattice spacing errors in the spatial and temporal derivatives removed—all links are tadpole improved by dividing by u_0, the average link in the Landau gauge:

$$
\begin{aligned}
a\mathcal{L}_F &= \psi_t^\dagger\psi_t - \psi_t^\dagger\left(1-\frac{a\delta H}{2}\right)_t\left(1-\frac{aH_0}{2n}\right)^n_t \\
&\times\frac{U^\dagger_{4,t-1}}{u_0}\left(1-\frac{aH_0}{2n}\right)^n_{t-1}\left(1-\frac{a\delta H}{2}\right)_{t-1}\psi_{t-1}\,,
\end{aligned}
\tag{1}
$$

$$
H_0 = -\frac{\Delta^{(2)}}{2m}\;,\;\delta H = \frac{a^2\Delta^{(4)}}{24m} - \frac{a\left(\Delta^{(2)}\right)^2}{16nm^2}\,. \tag{2}
$$

n is the stability parameter chosen to satisfy $n > \frac{3}{ma}$. $\Delta^{(2)}$ is the gauge-covariant lattice Laplacian, and $\Delta^{(4)}$ is the gauge-covariant lattice quartic operator ($\sum_i D_i^4$).

The gauge action is tadpole improved with leading finite lattice spacing errors removed by rectangles:

$$
\begin{aligned}
S_G &= \beta\sum_{pl}\frac{1}{3}Re\,Tr\,(1-U_{pl}) \\
&\quad - \frac{\beta}{20u_0^2}\sum_{rt}\frac{1}{3}Re\,Tr\,(1-U_{rt})\,.
\end{aligned}
\tag{3}
$$

The 'kinetic' meson mass is defined by

$$
E(\boldsymbol{p}) - E(\boldsymbol{0}) = \frac{\boldsymbol{p}^2}{2M_{kin}}\,, \tag{4}
$$

where $E(\boldsymbol{p})$ is the simulated meson energy.

1.2. Perturbative lattice NRQCD

The Feynman rules are derived from the Lagrangians of Eqs. (1) and (3) by making the replacement $U_\mu(x) \to \exp[iagA^a_\mu(x)T^a]$. The gluon propagator follows from the quadratic piece of the gauge action in Eq. (3)—we take the piece proportional to $\delta_{\mu\nu}$ in this paper.

The continuum and lattice decay constants in one-loop perturbation theory are related by $f_V = Z_{match}f_{V,latt}$, where $Z_{match} = 1 + g^2\left(-\frac{2}{3\pi^2} - (\delta V + \delta Z)_{latt}\right)$. Note that a linear infrared divergence cancels between the continuum and lattice perturbative shifts. Fig. 1 shows the results of the one-loop calculation. The shown errors are estimates of the extrapolation errors. All

*Presented by B.D. Jones at Lattice '98, 13–18 July.

Table 1
M_{pert} versus M_{kin} for the runs nearest the charm and bottom regions respectively.

β	a(fm)	$ma[n]$	$M_{kin}a$	$M_{pert}a$ w/o tad imp	$M_{pert}a$ w tad imp	M_{kin}(GeV)
7.2	.240(3)	1.6[3]	3.37(6)	2.89(7)	3.60(7)	2.77(6)
7.3	.205(3)	1.5[3]	3.20(5)	2.64(6)	3.37(6)	3.08(6)
7.4	.178(3)	1.4[3]	3.00(6)	2.39(6)	3.15(6)	3.32(9)
7.2	.198(2)	4.4[2]	9.07(21)	9.47(68)	8.98(68)	9.05(23)
7.3	.174(3)	4.3[2]	8.74(20)	9.17(61)	8.74(61)	9.91(28)
7.4	.151(2)	3.5[2]	7.05(20)	7.22(38)	7.06(38)	9.20(29)

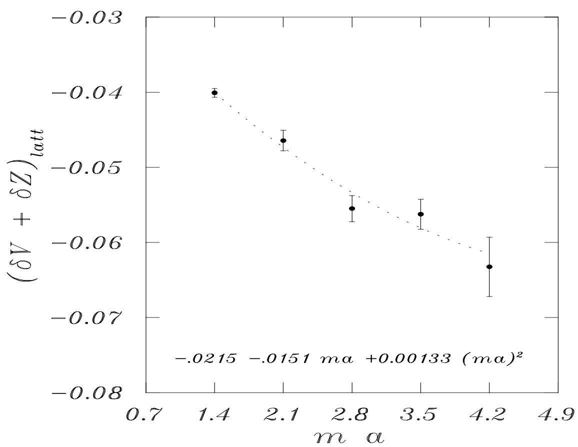

Figure 1. Perturbative lattice NRQCD one-loop contribution to the matching of the heavy-heavy vector current. These results must be multiplied by g^2.

one-loop integrals are performed by VEGAS [7] in this paper.

The "perturbative" meson mass is defined by $M_{pert} = 2(mZ_m - E_0) + E_{sim}$. Table 1 shows the simulation parameters near the physical regions and compares M_{pert} and M_{kin}. The lattice spacing is fixed by the S–P splitting: 458 MeV, a boosted coupling is used: $g^2 = \frac{5}{3}\frac{6}{\beta u_0^4}$, and $u_0 = 1 - \frac{g^2}{4\pi}u_0^{(2)}$ is used to define $u_0^{(2)}$.

1.3. Decay constants

The asymptotic form of a meson propagator is

$$G(\boldsymbol{p},t) \xrightarrow[t-t_0\to\infty]{} |\langle 0|J(0)|\boldsymbol{p}\rangle|^2 \times \exp[-E(\boldsymbol{p})(t-t_0)]\,, \quad (5)$$

where $J(\boldsymbol{x},t) = \chi_x\Gamma_x\psi_x$ is a non-relativistic current with $\Gamma_x = \Omega_x\gamma_x$, where Ω_x interpolates the meson of interest and γ_x is a smearing operator chosen in a gauge-invariant fashion: $\gamma_x = [1+\epsilon\Delta^{(2)}(x)]^{n_s}$. We set $\epsilon = 1/12$ and tune the smearing parameter n_s to maximize the overlap with the state of interest. We find the range 7–30 for n_s to be sufficient, with the P-wave requiring about twice as much smearing as the S-wave and the smearing parameter increasing for decreasing quark mass.

The above matrix element for a vector at rest is related to its decay constant f_V through $\langle 0|J(0)|V\rangle = \frac{f_V M_V}{\sqrt{2M_V}}$, where a non-relativistic norm is used.

Finally, note that simulations are performed with an order v^2 classically improved current. The improved interpolating operator for a non-relativistic vector meson is given by

$$\Omega_V^{imp} = \sigma_i + \frac{1}{8m^2}\left(\Delta^{(2)\dagger}\sigma_i + \sigma_i\Delta^{(2)}\right) - \frac{1}{4m^2}\left(\boldsymbol{\sigma}\cdot\boldsymbol{\Delta}^\dagger\right)\sigma_i\left(\boldsymbol{\sigma}\cdot\boldsymbol{\Delta}\right), \quad (6)$$

where $\boldsymbol{\Delta}$ is the symmetric lattice gauge-covariant derivative.

2. RESULTS AND DISCUSSION

The data sample includes 1600 quenched gauge field configurations at $\beta = 7.2$ and 7.3 ($8^3 \times 14$), and 1200 configurations at $\beta = 7.4$ ($10^3 \times 16$). Multiple sources along the spatial diagonal are used to measure the local-smeared meson correlators with the number of smearing steps optimized to have the best overlap with the state of interest. All plots include bootstrap errors using twice as many bootstrap ensembles as there are configurations.

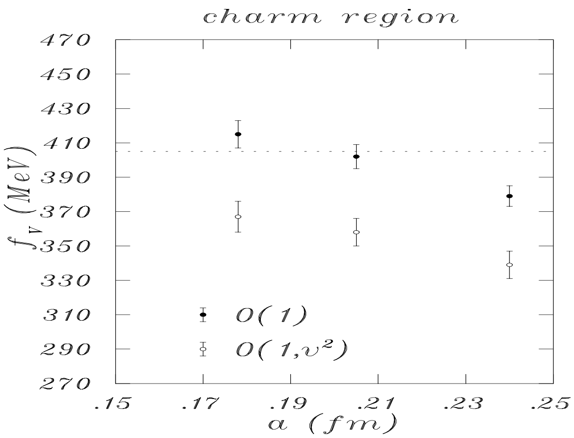

Figure 2. Scaling behavior of the charm decay constants including the perturbative matching. The dotted line is the experimental result.

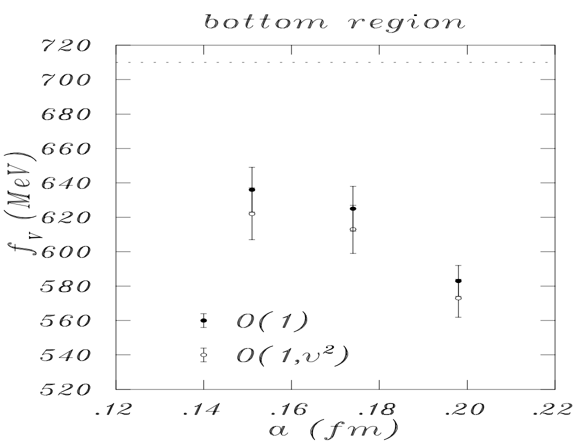

Figure 3. Scaling behavior of the bottom decay constants including the perturbative matching. The dotted line is the experimental result.

Figs. 2–4 show our main results. Note the 10% underestimations (order v^2 improved data) as expected from the previous work on the spin splittings. Also note the approximate $\sqrt{M_V\,a}$ dependence. Shortly after the discovery of charm, Yennie [8] noticed this same dependence from empirical data:

$$\frac{\Gamma^V_{e\bar{e}}}{e_q^2} \sim \text{constant} \sim 12\ \text{keV} \tag{7}$$

for light through heavy ground-state vector mesons (e_q is the quark charge in units of e). This is the same as our data since the leptonic

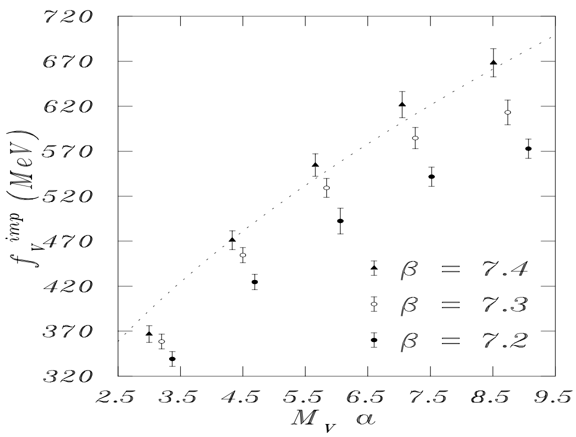

Figure 4. Meson mass dependence of the order v^2 improved decay constant including the perturbative matching. The dotted line is proportional to $\sqrt{M_V\,a}$.

width is proportional to $e_q^2 \frac{f_V^2}{M_V}$. A final note is that a *linear* (*Coulomb*) potential implies a *constant* (*linear*) dependence on the meson mass for the decay constant, so our data is consistent with a superposition of the two potentials.

ACKNOWLEDGMENTS

The authors thank N. Shakespeare and H. Trottier for discussions. This work is supported by the Natural Sciences and Engineering Research Council of Canada.

REFERENCES

1. G.P. Lepage et al., Phys. Rev. D **46**, 4052 (1992).
2. C.T.H. Davies et al., Phys. Rev. D **50**, 6963 (1994).
3. C.T.H. Davies et al., Phys. Rev. D **52**, 6519 (1995).
4. H.D. Trottier, Phys. Rev. D **55**, 6844 (1997).
5. C.T.H. Davies and B.A. Thacker, Phys. Rev. D **48**, 1329 (1993).
6. G.T. Bodwin et al., Phys. Rev. Lett. **77**, 2376 (1996).
7. G.P. Lepage, J. Comput. Phys. **27**, 192 (1978).
8. D.R. Yennie, Phys. Rev. Lett. **34**, 239 (1975); J.J. Sakurai, Physica A **96**, 300 (1979).